Development of a Limited-Area Model for Operational Weather Forecasting around a Power Plant: The Need for Specialized Forecasts

C. F. BALSEIRO, M. J. SOUTO, AND E. PENABAD

Group of Nonlinear Physics, Faculty of Physics, University of Santiago de Compostela, Santiago de Compostela, Spain

J. A. SOUTO

Department of Chemical Engineering, University of Santiago de Compostela, Santiago de Compostela, Spain

V. PÉREZ-MUÑUZURI

Group of Nonlinear Physics, Faculty of Physics, University of Santiago de Compostela, Santiago de Compostela, Spain

(Manuscript received 7 May 2001, in final form 11 March 2002)

ABSTRACT

A hydrostatic meteorological model, ''PMETEO,'' was developed for short-range forecasts for a high-resolution limited area located in the northwest region of Spain. Initial and lateral boundary conditions are externally provided by a coarse-mesh model that has much poorer horizontal and vertical resolution than the fine PMETEO grid. Limitations of limited-area models due to lateral boundary conditions are widely known, given that they can have a large impact on the evolution of the predicted fields through the propagation of errors into the interior of the domain. The guidelines to minimize this problem depend on the particular circumstances of the model application. In this case, a specific treatment of the initial and time-dependent boundary conditions is presented that obtains the best accuracy in the model results, because PMETEO is run operationally to predict air quality levels around a power plant.

1. Introduction

The need for high-resolution mesoscale meteorological information is growing rapidly. For example, local industries or governments interested in air quality problems require high temporal and spatial resolution for weather forecasting, as well as model simulations that are completed in a reasonable amount of time. In recent years, numerical weather forecast systems have been used at fine horizontal resolutions ranging from 1 to 10 km. However, the specific data requirements needed to initiate accurately the meso-β weather systems that handle detailed short-range forecasting are not well established. There are a wide variety of sources of forecasting errors that may make a particular limited-area model unsuitable for a specific application. These errors may be due to limitations in physical process parameterizations, numerical algorithms, or surface forcing representation. These limitations can be addressed through a variety of well-known methods. However, a significant limitation in the accuracy of model results is the inability to specify proper initial and boundary conditions for high-resolution model simulations. Numerous studies have demonstrated that initial and boundary conditions can have a large impact in the evolution of the predicted fields, through the propagation of errors (Shapiro and O'Brien 1970; Perkey and Kreitzberg 1976; Warner et al. 1997).

A solution to problems due to inaccurate lateral boundary conditions (LBC) in limited-area models must involve an understanding of the nature of the problems and knowledge to mitigate their negative effects for each particular model application. A desired characteristic of interpolation schemes employed in the specification of boundary conditions for nested models is their ability to allow all resolvable waves to propagate across the coarse–fine-grid interface with minimal distortion so that compatibility between the solutions computed on the different grids can be maintained. The model users should employ specific modeling strategies that minimize the LBC effects (Alapaty et al. 1998). However, under certain situations, computing-resource factors play an important role in this decision. The same situation occurs when preparing the initial conditions. Each model has a particular procedure to perform horizontal interpolation of coarse-resolution data to a fine

Corresponding author address: C. F. Balseiro, Group of Nonlinear Physics, University of Santiago de Compostela, Campus Sur, 15782 Santiago de Compostela, Spain.
E-mail: cfb@cesga.es

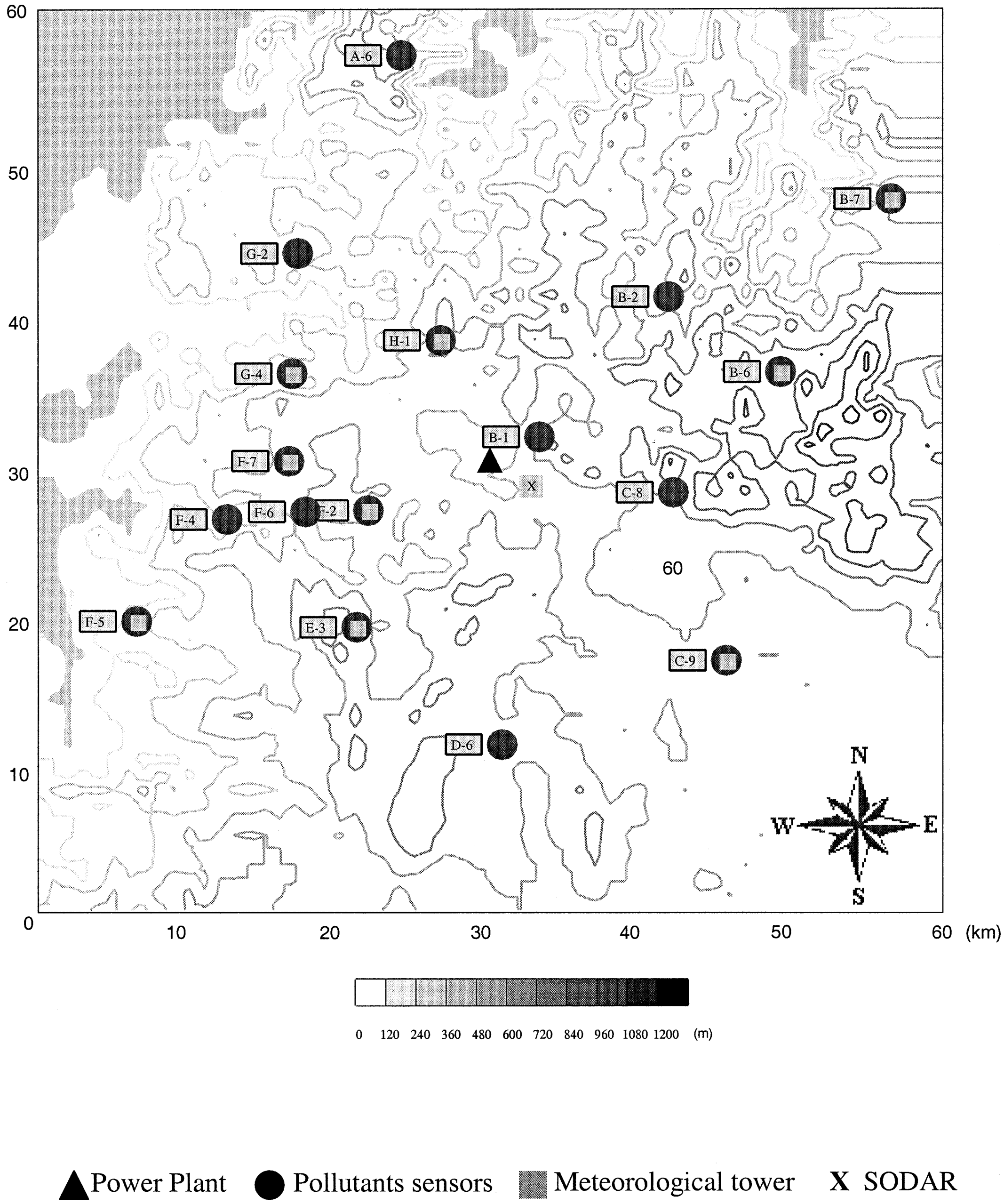

FIG. 1. Topography of the area under study in northwestern (Galicia) Spain: (gray zones) sea areas in the north and west, (squares) meteorological towers, (circles) GLC stations, (X) the sodar in A Mourela, and (black triangle) As Pontes 1400-MW power plant.

resolution. For example, the fifth-generation Pennsylvania State University–National Center for Atmospheric Research (NCAR) Mesoscale Model (MM5) uses a 16-point, two-dimensional overlapping-parabolic interpolation method (Dudhia et al. 2000). In recent years, special efforts have been made to improve the initial conditions by adding all available measurements. With this aim, four-dimensional data assimilation variational techniques have been applied to medium- and long-range forecasts by, for example, the European Centre for Medium-Range Weather Forecasts and NCAR. The use of these approaches implies high computational expenses, usually beyond the capabilities of a particular industry.

An air pollution control system for prediction of mesoscale plume transport has been applied since 1995 to the As Pontes Power Plant, As Pontes, Spain (Souto et al. 1998; Fig. 1). Plume transport is extremely sensitive to meteorological fields, and its forecast requires a highly precise meteorological prediction. To achieve this goal, a limited-area hydrostatic meteorological model, ''PMETEO,'' has been developed to provide a cost-effective high-resolution meteorological forecast with a grid mesh of 2 km.

In this paper, specific modeling strategies developed to produce specialized forecasts using PMETEO are presented, especially those concerning the minimization of negative effects of initial conditions and LBCs on forecasts. PMETEO is used for operational forecasting in an industry in which computing resources play an important role in our decisions. This paper is divided into two main parts. Section 2 introduces PMETEO and the initialization procedure used by the model, as well as the different boundary conditions considered. Section 3 shows the accuracy of this model to forecast the meteorological conditions for three consecutive days in May of 1997. Conclusions are presented in section 4.

2. Meteorological model

The PMETEO meteorological dynamical model is a three-dimensional time-dependent mesoscale hydrostatic model based on a finite-difference solution of the hydro-thermodynamical equations (Pérez-Muñuzuri 1998; Souto et al. 1996, 1998; Souto et al. 1999, 2001). A terrain-following coordinate system is used to put the topography into the model (Pielke and Martin 1981; Enger 1990). A first-order local closure is applied to solve the governing diffusion equations. When the layer is stably stratified, a parameterization based on the Richardson number as suggested by Blackadar (1979) was used. On the other hand, when the atmospheric boundary layer is unstably or neutrally stratified, O'Brien's (1970) cubic polynomial approximation is used. To apply this profile formulation, the depth of the planetary boundary layer (PBL) must be known.

During convective conditions, the depth of the PBL is usually associated with an inversion, and it is calculated as suggested by Deardoff (1974), by a prognostic equation that depends mainly on the surface heating (Pielke 1984). The expression of Smeda (1979), who proposed that the growth of the stable layer is proportional to the stress induced by the wind near the surface, is used. The height calculated by this expression during the transition from convective to stable conditions could be considered to be a fictitious height during the time when the stable layer near the surface develops and becomes well established, so the model provides a value for the PBL during all the periods of simulation. The vertical turbulent fluxes, which take into account the vertical mixing of the atmosphere, are parameterized depending on the stability of the layer being simulated. In this process, the model calculates the turbulence parameters that define the atmospheric stability and the depth of the PBL. These turbulent parameters have been calculated using an iterative procedure, as shown in Berkowicz and Prahm (1982), based on wind speed and temperature values at two different levels near the ground (San José 1991). In this case, the lowest level was chosen at 3 m, the first vertical layer of the grid model, and the second level was chosen at at 10 m above the ground.

The prognostic equations are solved using a forward-in-time, upstream-in-space finite-difference scheme for the advection terms. For the vertical diffusion terms, a semi-implicit scheme with a weight of 75% on the next step is used. The remaining spatial derivatives are solved with a forward-in-time, centered-in-space scheme. Coriolis terms are evaluated by an implicit scheme, and radiative terms are solved by using an explicit scheme. By using an upwind scheme for the advection terms, nonlinear waves appear, disturbing the solution. Although an eddy parameterization of the horizontal turbulent fluxes has been selected to minimize these effects (Tag et al. 1979), a 2D filtering based on the averaging of the prognostic variables with the nearest neighbors with some factor α (Haltiner and Williams 1980) has also been applied. We have used 40 vertical levels beginning at 3 m above the ground and spaced logarithmically until reaching the top of the model at 7000 m. There are 31×31 grid points in each vertical level, with a horizontal grid spacing of 2 km.

A full meteorological model should parameterize the subgrid-scale cloud dynamics to take into account their influence in the atmospheric flow and pollutant transport (Gimson 1997). To avoid these extensive calculations that require the use of high-performance computers not available in an industrial plant, a method for cloud-cover dynamics (average cloud absorption) was developed based on nonlinear chaotic predictions (Pérez-Muñuzuri 1998). In this method, techniques of nonlinear analysis are applied to a time series of 0.5-h cloud absorption values (averaged in space for the area of interest) obtained from infrared Meteosat images for 24-h forecasting. Later on, the obtained time series of average cloud absorption are used by PMETEO. This nonlinear method reveals the possibility of short-term prediction of atmospheric parameters whose dynamics would make it very difficult to obtain a prognostic equation by other means (Pérez-Muñuzuri and Gelpi 2000).

The continuity equation and the hydrostatic pressure relation are integrated using an explicit finite-difference scheme to obtain the vertical component of the wind, as well as the scaled pressure. To avoid spurious effects due to initialization, the model is run for 1 h without time-dependent forcing terms.

a. Initial conditions

The initial conditions applied in this version of the PMETEO model are provided by the Spanish National Weather Service (INM), in terms of a 24-h meso-α forecast of wind, temperature, and relative humidity at seven constant pressure levels (1000, 975, 950, 925, 850, 700, and 500 hPa), plus the surface level, for 24 points on

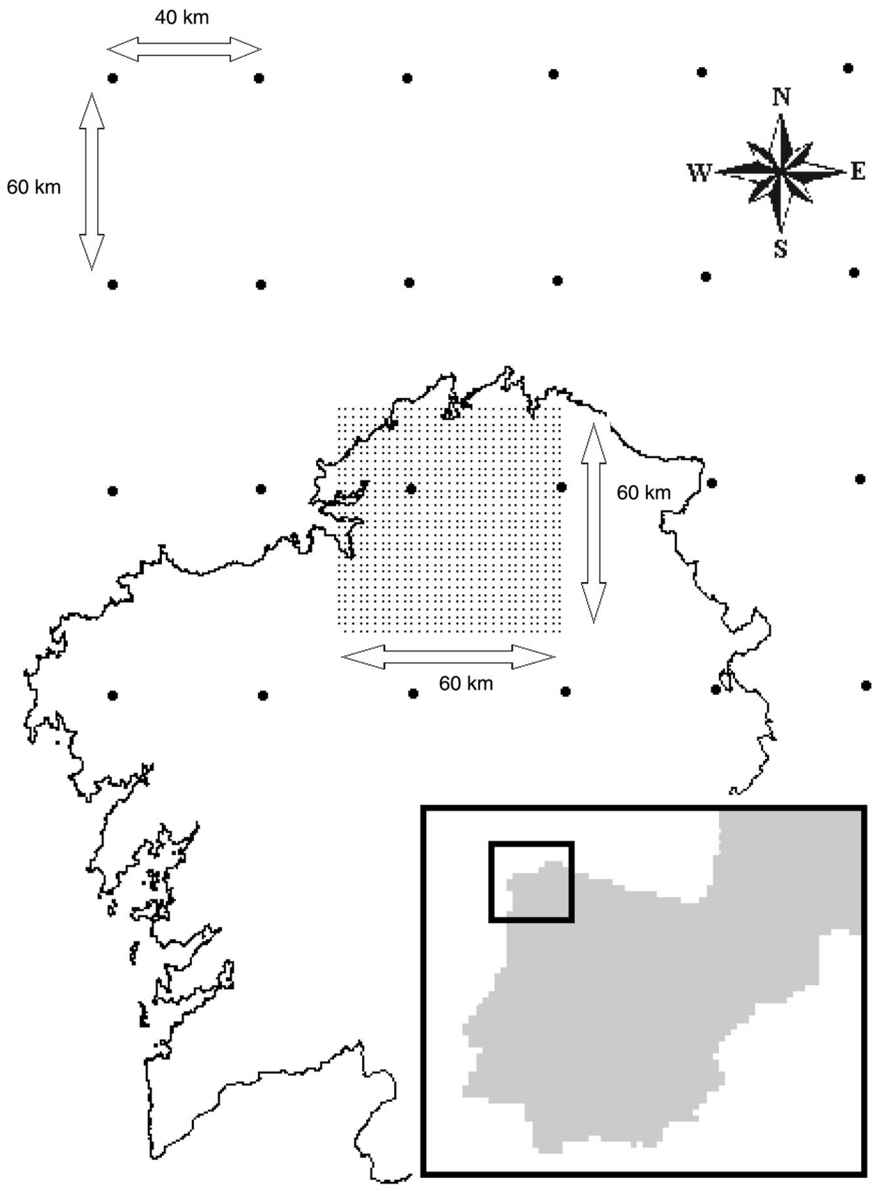

FIG. 2. Coarse-mesh grid used by the INM model compared with PMETEO fine-mesh grid.

a 0.5° horizontal grid from the High-Resolution Limited-Area Model (Källen 1996). Figure 2 shows the distribution of these 24 points in comparison with the location of the finer mesh grid used in northwestern Spain. This information is distributed in periods of 3 h; the first period of this forecast is used by PMETEO as the initial conditions of each simulation, and the following periods establish the evolution of the boundary conditions during the 24-h simulation.

Because of the difference between the coarse grid size used by the meso-α model ($\approx$50 km) and the finer mesh size used by PMETEO (2 km), only two sites are actually available over the area of interest. The pressure is quadratically interpolated to the finer mesh grid points at each of the pressure levels provided by INM, and temperature and relative humidity are linearly interpolated. Values of the wind component are quadratically interpolated because the linear interpolation technique was only slightly worse, but schemes that introduce a weighting bias that depends on wind direction, or the use of data from the nearest observing site, were significantly worse. These different interpolation schemes were chosen following the results obtained by Ludwig et al. (1999), Goodin et al. (1979), and Mathur and Peters (1989). For vertical interpolation, the wind components are linearly interpolated, and the rest of variables are interpolated using a cubic spline. This procedure is repeated for each of the eight periods provided by the INM, so the boundary values of the dependent variables are known at each 3-h period and can be used to define appropriate boundary conditions that evolve in time, as shown below.

The mesoscale initial data are sparse. As was mentioned above, the model was initialized well before the desired forecast period to allow for the model internal dynamics to spin up mesoscale structures, which are responsible for the large-scale and local forcing. Thus, the model is run for 1 h during which no time-dependent forcing terms are permitted to occur. This period of time can be shortened if the difference between two consecutive integration steps is lower than a certain threshold for any prognostic variable.

The thermal inversions observed at the coarse INM profiles must be adequately converted to local temperature profiles because the input data are georeferenced to the sea surface level whereas PMETEO uses a finer terrain-following coordinate system. Only two global model points are included into the small domain. We checked to see whether a thermal inversion existed for these points. If one did, we characterized it by its height, by the temperature decrease associated with it, and by the altitude corresponding to this point. With this information, we generate the inversion in the small domain points by correcting the interpolated profile with an inversion located at one-half of the original height of the inversion, with one-half of the temperature indicated by the INM, taking into account the altitude of each point. Figure 3 shows a comparison between both profiles. Note that the INM profile shows an inversion caused by cooling at approximately 200 m; because the PMETEO profile corresponds to a grid point in the finer mesh grid located at 700 m over the sea surface, the interpolation described above would ignore that inversion. This new profile represents more adequately the real meteorological situation for that grid point.

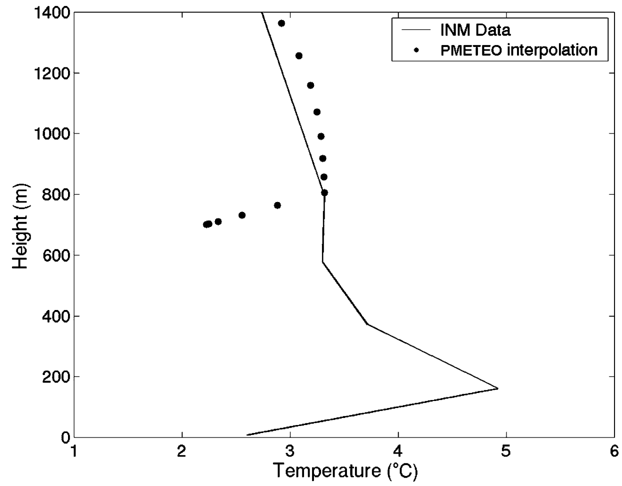

FIG. 3. (solid line) Temperature profile given by the INM compared with (dashed line) the interpolated one used by PMETEO.

b. Boundary conditions

Conditions at the boundaries of the domain must allow for not only the external conditions, but also the mathematical conditions that allow for a correct numerical solving of the model. In this model, the wind at the ground surface is considered to be zero. The derivatives of the horizontal wind components at the top boundary are set to zero (i.e., homogeneous geostrophic wind). The vertical gradient of potential temperature and the specific humidity at the model top are assumed to be constant. The temperature at the ground is calculated by means of a force–restore method (Deardorff 1978), and a specific sea surface physics parameterization (Pérez-Muñuzuri 1998) has been used to achieve a better description of the circulating flows at the coastline. The relative humidity at the ground surface is calculated by a method proposed by McCumber and Pielke (1981), which mainly depends on the surface temperature.

Lateral boundary conditions are interpolated in time by using a cubic spline method from the interpolated three-dimensional meteorological fields provided by INM every 3 h. Then, for each time step, LBCs for the spatial derivatives at each level are supplied by INM at the inflow boundaries, and zero gradient is applied at the outflow boundaries for the horizontal wind components and relative humidity. For better results, potential temperature LBCs are always from INM, regardless of flow direction. In addition, a numerical filter near the lateral boundaries was applied to damp advective and wave disturbances that are expected to appear in hydrostatic models (Chen 1973). In this case, when air flows from the outside to the inside of the grid (inflow boundaries), the relaxation term $-K_b(\phi - \phi_0)$ was added to the prognostic equations. Here, K_b is called the relaxation coefficient (Davies 1983),

$$K_b = \begin{cases} K_{b_0}\{1 + [2 + (i - i_b)(n_b - 1)^{-1}]^2\}^{-1} & |i - i_b| \le n_b - 1 \\ 0 & |i - i_b| > n_b - 1, \end{cases} \tag{1}$$

and ϕ_0 is the value obtained by interpolation of the correspondent ϕ variable from the INM dataset. As well, K_{b_0} is the maximum value of the relaxation coefficient (equal to 0.0033 s^{-1}), n_b is the number of grid points near the lateral boundary where the relaxation is being applied, and i_b is any grid point within that area.

A traditional way to reduce the LBC error has been simply to move the lateral boundaries sufficiently far

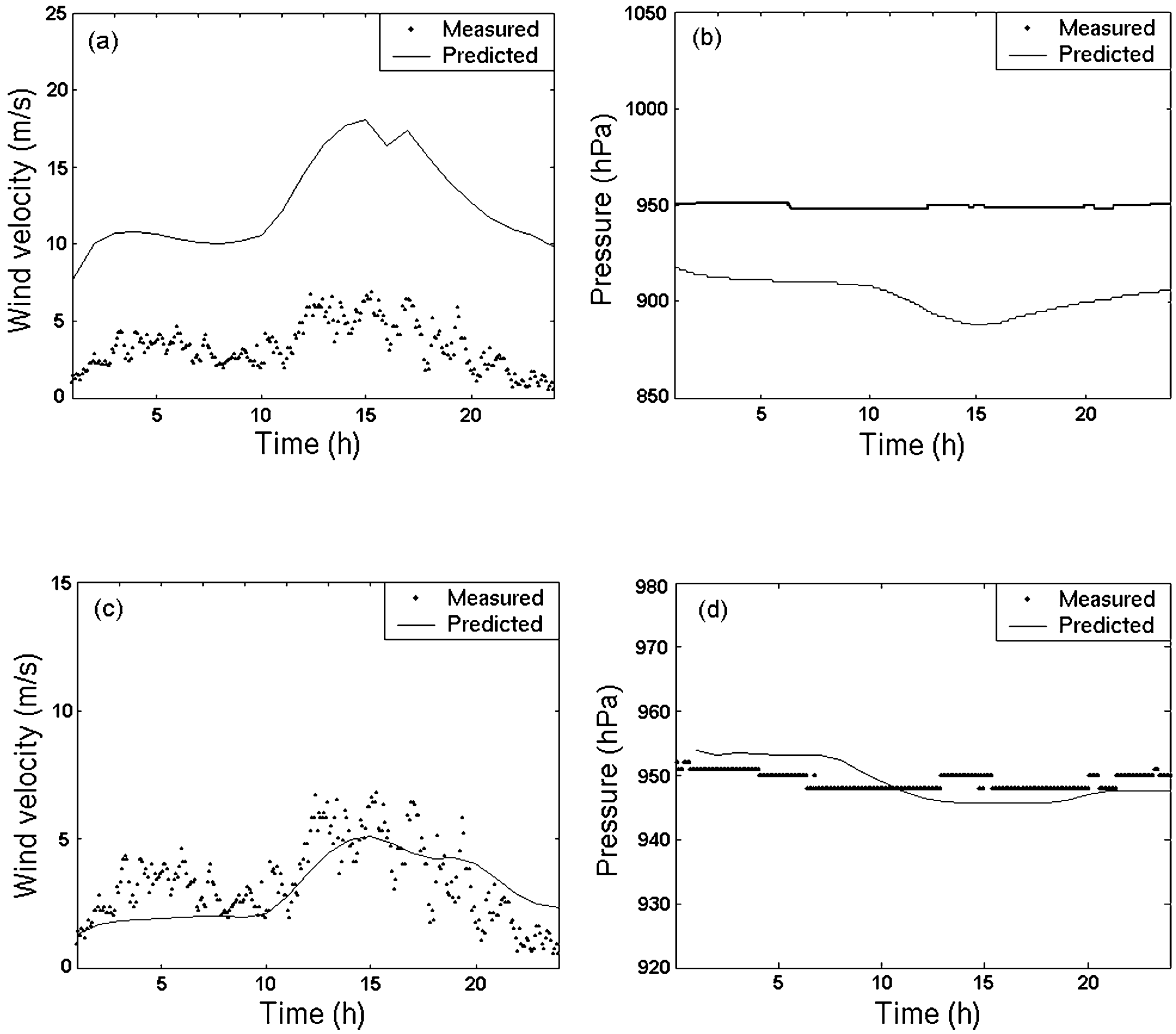

FIG. 4. Wind velocity and pressure time evolution in (grid center) A Mourela station for 23 May 1997 (a), (b) before and (c), (d) after the new pressure interpolation.

from the area of meteorological interest that their effect is within acceptable limits during the period of an integration. In this case, because of the high computational expenses, this option was not used.

The vertical interpolation of surface pressure is a very complicated problem, especially when going from coarse grids to fine grids in areas of sharp or complex terrain. Much work has already been done on this problem in relation to obtaining regional-analysis first-guess fields from global models. In this case, the top and surface pressure are also interpolated in time from the given values provided by the INM for every 3 h. Then, the hydrostatic equation is integrated twice using an explicit Euler method, from the sea level to the top boundary $p_1(z)$, and vice versa $p_2(z)$, to obtain the pressure at each grid point within the 3D grid. To avoid the accumulation of errors due to the integration method either at the top or at the surface pressure values, a single pressure profile $p(z)$ is proposed for each grid point, calculated by means of a linear weighted combination of both profiles with function $w(z)$, so

$$p(z) = w(z)[p_1(z) - p_2(z)] + p_2(z) \tag{2}$$

$$w(z) = [1 - bz(\log z)^{-1}]^2, \tag{3}$$

where (3) was obtained after fitting to different typical meteorological situations in the area of interest, with $b = 1.26 \times 10^{-3}$. Note that $w(z)$ is equal to 1 near the sea level, so $p_1(z)$ is more significant at this level, whereas the opposite behavior occurs at the top of the model $[p(z) \approx p_2(z)]$. Figure 4 shows the time evolution of wind speed and pressure obtained by the model in comparison with real data measured in the A Mourela, Spain, station at 365-m height above the sea level, when only

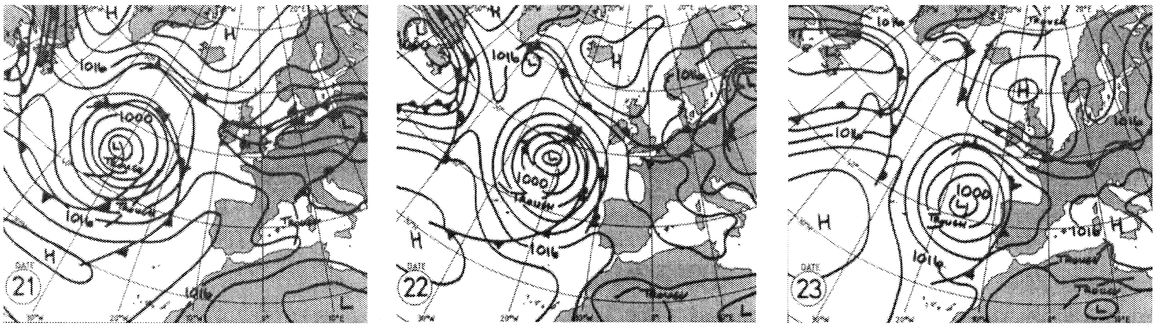

FIG. 5. Synoptic maps for 21–23 May 1997.

$p_1(z)$ is used (Figs. 4a,b) instead of applying the $p(z)$ profile (Figs. 4c,d).

3. Results

The area under consideration is located in northwestern Spain and is characterized by steep hills and sea inlets bathed by the Atlantic Ocean and is surrounded by cliffs that affect the wind direction. Topography of the area (60 km × 60 km; shown in Fig. 1) has a central point at the As Pontes Power Plant, where a continuous gas plume is exhausted at 356.5 m above ground level and 688.4 m above sea level. This area is located between 43°9′ and 43°40′N and 7°36′ and 8°12′W. The top of the region is the Serra do Xistral, 1036 m above sea level.

The accuracy of the initial and the boundary conditions implemented in the PMETEO code are checked daily at the As Pontes Power Plant, where the meteorological model is being used to forecast the most significant plume impacts. The real-time meteorological and air pollution network (Fig. 1), with its grid of nine meteorological towers, one Remtech, Inc., PA-3 sodar, and 17 sulfur dioxide (SO_2) ground-level-concentration

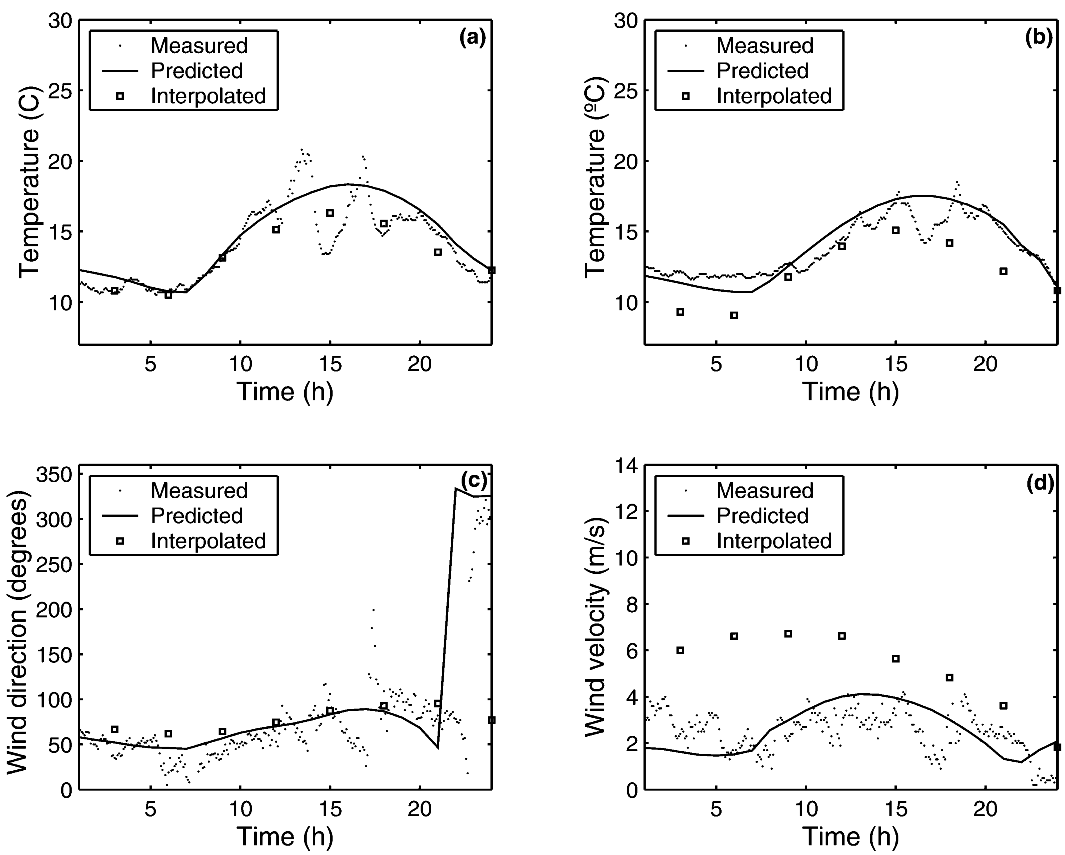

FIG. 6. Measured, PMETEO-predicted, and interpolated 10-m surface temperature at (a) F5 and (b) B7 stations, and (c) wind direction and (d) wind velocity at the A Mourela station, 21 May 1997.

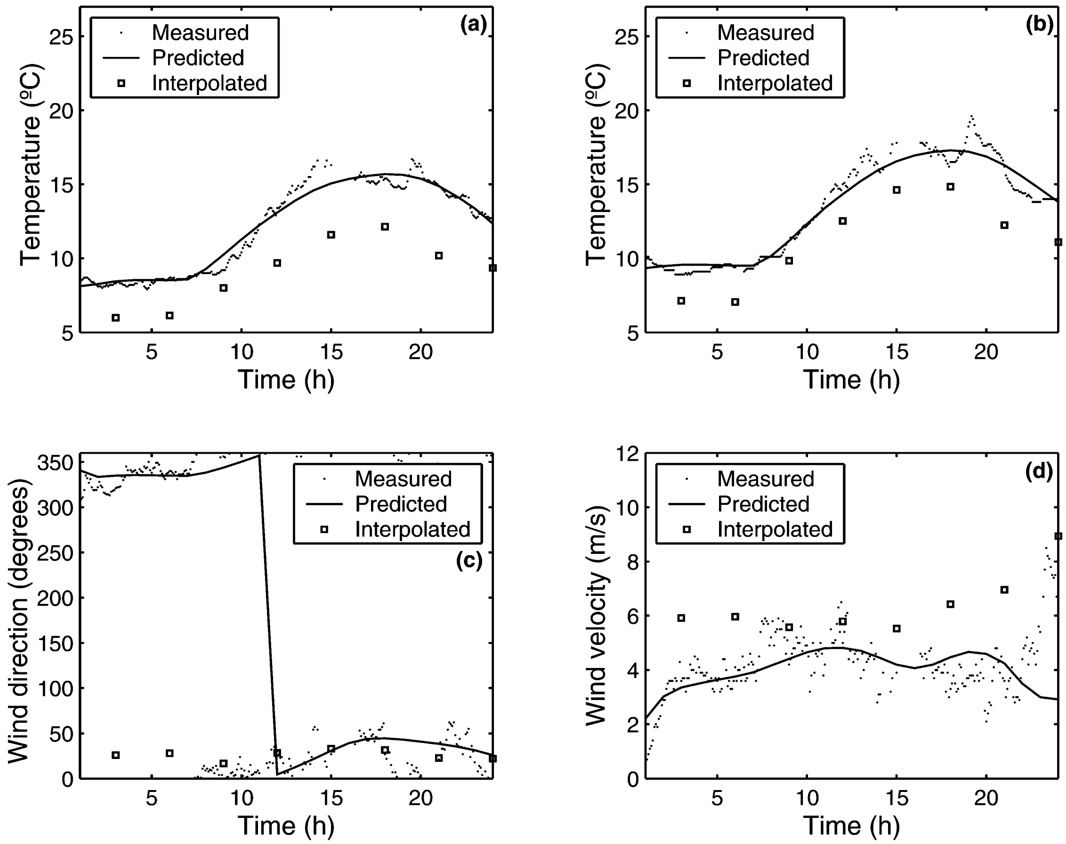

FIG. 7. Measured, PMETEO-predicted, and interpolated 10-m surface temperature at (a) B6 and (b) E3 stations, and (c) wind direction and (d) wind velocity at the E3 station, 22 May 1997.

(GLC) remote stations, provides continuously averaged data to a database system. Nevertheless, in this study we have selected 3 days from 21 to 23 May 1997 for research purposes. During these days, a low pressure area initially located near the Azores Islands slowly approached to the Iberian Peninsula and brought an overcast sky and scattered showers to this area (0.2, 0.0, 0.8 mm for 21, 22, 23 May 1997, respectively), which were frequently accompanied by moderate southwest winds (Fig. 5).

In the next set of figures (Figs. 6–9), comparison between PMETEO-predicted values of surface temperature, horizontal wind velocity, and horizontal wind direction (continuous line) and measurements (dots) is shown. We also did a direct interpolation of the coarser-resolution INM data to the inner grid (squares).

On 21 May 1997, warm temperatures ranging from 10° to 20°C were measured. As observed in Fig. 6a (F5 station), measured values of the temperature show a sharp decrease at 1500 local time due to the pass of a cloudy air mass that produces a decrease in the solar radiation that reaches the surface. This effect is also observed in Fig. 6b (B7 station), but approximately 1 h later because of its location (more easterly than the previous station; see Fig. 1). The evolution of the forecast temperature during 21 May (see Fig. 6) adequately reproduces the general trend of the day; however, the observed sudden decrease of the temperature is not correctly solved by the model. At F5 station, the interpolated INM temperature is similar to real and forecast values; at B7 station, PMETEO results considerably improve the temperature forecast during all the simulation periods. Although PMETEO accounts for a cloud coverage parameterization that varies with time (Pérez-Muñuzuri 1998), it only takes into account an average value over the area of interest, which favors the smoothed temperature time series behavior obtained with the forecasting model.

On the other hand, the high pressure area situated over the Atlantic Ocean produces light southwesterly winds. In this case, the model correctly reproduces the wind direction evolution for day 21, with a constant value of southwestern winds during all of the morning. In addition, the model is able to predict the drift evolution of the flow to the west measured during the afternoon and the sudden change to the southeast at night because of the front associated with the low pressure center. The interpolated INM values did not reproduce this change and also obtained very high wind velocity values.

During 22 May, the front associated with the low pressure center entered the simulated area, giving rise to southern winds and a temperature decrease, especially

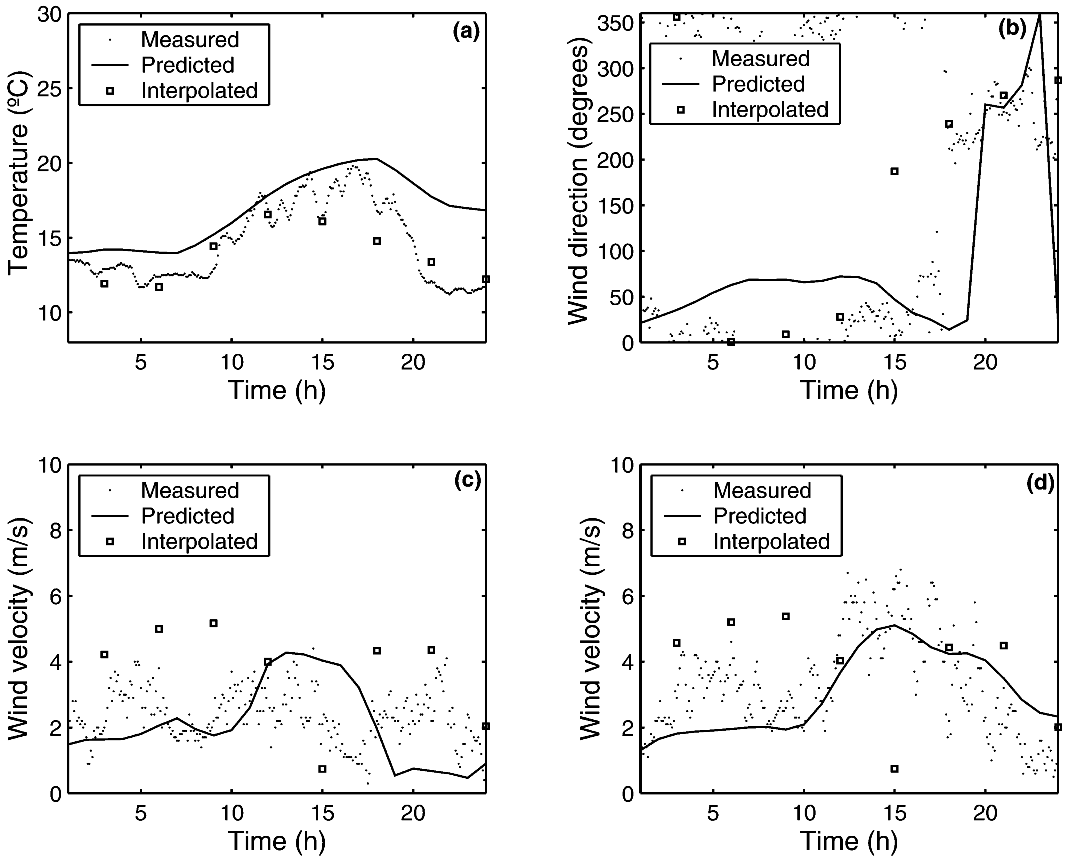

FIG. 8. Measured, PMETEO-predicted, and interpolated 10-m (a) surface temperature and (b) wind direction at the A6 station, and wind velocity at the (c) A6 station and (d) A Mourela station, 23 May 1997.

at night, with measured values from 8.0° to 20°C. In Figs. 7a,b, the time evolution of the temperature at two stations at different heights (B6 at 846 m above sea level, and E3 at 703 m above sea level) is compared. At the B6 station, temperatures range from 8.0° to 15.5°C, and at the E3 station the temperatures range from 9.5° to 17.5°C. PMETEO predicted very well these different temperatures, mainly because of the correction of the interpolated temperature profile at the initial time and boundary conditions (described in section 2a). In this case, the interpolated INM values, even though they reproduced these temperature differences between the two stations, were worse than the PMETEO forecasts.

The time evolution of the boundary conditions included in the PMETEO model, supplied every 3 h, allows for an accurate prediction of wind direction and wind speed (as shown in Figs. 7c,d), especially the wind direction change from the southeast during the first hours of the day to the southwest measured during the rest of the day. Now again, the interpolated INM values did not represented this change, although the wind velocity and direction values agree reasonably well with measurements.

On 23 May, the front associated to the low pressure area was located within the limits of the area of simulation, giving rise to a rainfall increase and southern winds. During the afternoon, as the front passed and the low pressure center moved to lower latitudes, the wind direction changed from south to east and a wind velocity decrease was observed. Again, the PMETEO model was able to predict these changes with time, as observed in Fig. 8. Nevertheless, both forecasts, the PMETEO and the interpolated INM, were unable to reproduce the temperature decrease (5°C in less than 1 h) observed at the A6 station (Fig. 8a). The bigger PMETEO wind speed errors occurred during the first period (0–6 h), just when the front arrived at the area domain. In Figs. 8c,d, we can see that the real value has an increase from 2 to 4 m s^{-1} in only a few hours and then begins to decrease rapidly, and at 0700 the value is again about 2 m s^{-1}. PMETEO did not reproduce this high variability in the wind speed for this period, but for the following hours reproduced the values of wind velocity very well.

In Fig. 9, the comparison of forecast (continuous line), interpolated (squares), and sodar-measured (dots) vertical profiles of temperature (Fig. 9a), wind speed (Fig. 9b), and the vertical wind standard deviation σ_w (Fig. 9c) for 1500 UTC 23 May 1997 is shown. In Fig. 9a and Fig. 9b, a dashed line corresponding to the vertical profile at the INM point nearest to the sodar lo-

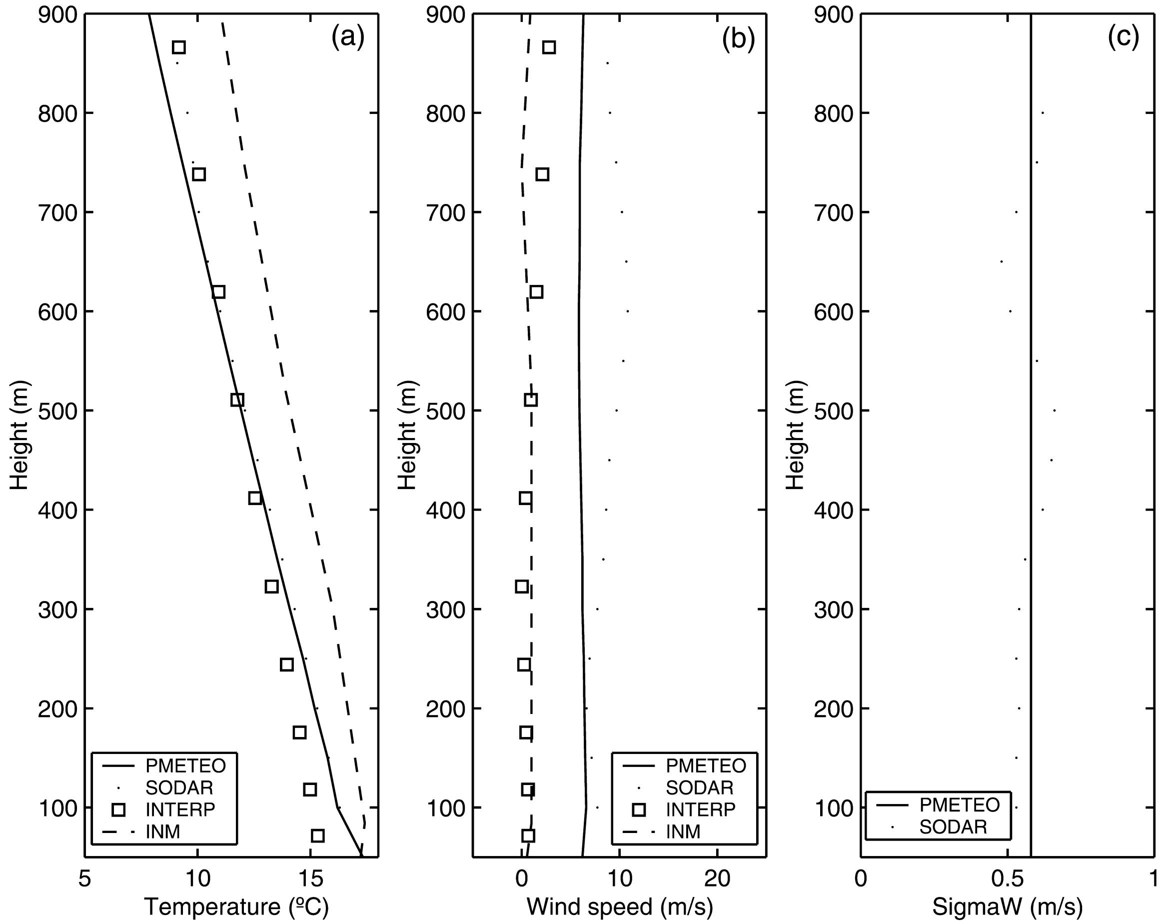

FIG. 9. Vertical profile comparison of (a) temperature, (b) wind speed, and (c) vertical wind standard deviation σ_w: (continuous line) PMETEO forecast, (squares) interpolated, and (dots) sodar measured for 1500 UTC 23 May 1997. (dashed line) The vertical profile at the INM point nearest to the sodar location.

cation is added. For both variables, the PMETEO forecasts obtained the best adjustment to real data. With the turbulence parameterizations developed in the PMETEO model based on surface variables, it is possible to obtain wind standard deviation values in all points of the high-resolution grid. These values will be used by the dispersion model to forecast the plume behavior and, therefore, the local plume impacts around the power plant (Souto et al. 2001). In Fig. 9c, a good agreement between σ_w-predicted and sodar-measured values is observed. Taking into account the specific application of the PMETEO model, the correct forecast of the temperature, wind speed, and, especially, the wind standard deviation vertical profile is a key issue given that they are the most important phenomena for plume rise and vertical plume growth calculation.

To complete the analysis of results presented above, a statistical estimation of the accuracy of PMETEO in comparison with measurements performed at the nine meteorological stations was made. The statistical measures used to test the meteorological model were the root-mean-square error (rmse) and the bias, defined as follows:

$$\text{rmse} = N^{-1}\sqrt{\sum_i [x(i) - x_{\text{pred}}(i)]^2}, \quad \text{and} \tag{4}$$

$$\text{bias} = N^{-1}\sum_i [x(i) - x_{\text{pred}}(i)], \tag{5}$$

where $x(i)$ and $x_{\text{pred}}(i)$ are values derived from observations and model predictions at the ith station, respectively, and N is the number of observations.

Table 1 shows 6-h-average values of these statistical parameters for the 3 days of simulation for three meteorological variables: wind speed, wind direction, and temperature and for the PMETEO and INM models. In general, the statistical index reflects the behavior described above. Thus, for example, for the third and fourth periods of 23 May, negative values of the bias in the PMETEO model show an overestimation of the temperature, which was described above as being caused by the failure of the model to reproduce the motion of

TABLE 1. The 6-h avg values for bias and rmse for the 3 days of simulation for three meteorological variables: wind speed, wind direction, and temperature for the PMETEO and INM models.

		PMETEO						INM					
	Time interval	Wind speed (m s^{-1})		Wind direction (°)		Temperature (°C)		Wind speed (m s^{-1})		Wind direction (°)		Temperature (°C)	
Date	(h)	Bias	Rmse	Bias	Rmse	Bias	Rmse	Bias	Rmse	Bias	Rmse	Bias	Rmse
21 May 1997	0–6	0.71	0.88	−4.26	8.09	−0.10	0.24	−2.79	1.29	−18.02	10.26	0.83	0.48
	6–12	−0.96	0.87	−12.68	11.45	−1.63	0.64	−3.43	1.40	−10.38	11.47	0.57	0.61
	12–18	−2.11	0.88	−5.32	14.03	−2.11	0.91	−3.31	1.21	1.34	12.21	0.11	0.75
	18–24	−0.76	0.54	2.16	24.77	−1.8	0.75	−2.38	0.86	31.00	21.58	0.04	0.57
22 May 1997	0–6	−1.35	0.99	−26.97	12.90	−1.31	0.60	−2.29	1.13	58.62	24.31	0.42	0.56
	6–12	−1.14	1.40	−21.45	11.46	0.37	0.70	−1.18	1.40	28.13	14.06	2.78	1.18
	12–18	−1.51	1.06	9.93	10.47	1.59	0.78	−1.34	1.10	9.81	9.82	3.73	1.48
	18–24	−1.69	1.00	21.43	18.63	−0.25	0.47	−2.29	1.27	22.87	14.01	1.91	0.90
23 May 1997	0–6	1.82	1.72	29.66	16.03	0.06	0.29	−0.03	1.43	15.25	13.21	2.07	0.83
	6–12	0.86	1.36	65.60	28.46	0.24	0.44	−0.97	1.36	28.09	16.25	2.29	0.95
	12–18	−0.45	1.53	8.25	28.48	−0.19	0.51	2.12	1.52	−19.14	28.50	2.63	1.12
	18–24	−2.73	1.13	37.51	39.97	−4.61	1.62	−2.30	0.95	−37.17	32.00	0.89	0.68

a cloudy mass of air over the area of simulation. In a similar way, the discrepancy shown between predictions made by the PMETEO model and measured wind direction during the first half of 23 May gives rise to high bias values. A comparision between the PMETEO and INM models is also shown in Table 1. Note that, in general, the PMETEO model presents lower errors than the INM model, as a consequence of its high spatial resolution and adequate physical parametizations, when model results are compared with meteorological surface station measurements.

4. Conclusions

A limited-area hydrostatic meteorological model, PMETEO, was developed for a high-resolution short-range forecast over a region of 60 km × 60 km located in northwest Spain. Initial and lateral boundary conditions are externally provided by a coarse-mesh model, with much poorer horizontal and vertical resolution than the fine PMETEO grid.

In this paper, specific modeling strategies to produce specialized forecasts using PMETEO are presented, especially those concerned with minimizing the negative effects of initial conditions and LBCs on forecasts. PMETEO is used for industrial operational prediction, so we should not forget that computing-resource factors play an important role in our decisions.

Comparison between PMETEO predicted values of surface temperature, wind velocity, and wind direction and measurements shows good agreement not only in the time-evolution forecast, but also in the vertical distribution. The need for this kind of high-resolution model for specific forecasts is demonstrated by making comparisons of PMETEO results with the data obtained from a direct interpolation of a coarse-resolution model.

Last, we emphasize that the whole system of forecast models that we have described has been succesful in forecasting the most important plume impact around the As Pontes Power Plant. These models have been run routinely since 1995 to provide forecasts under a large variety of meteorological conditions.

Acknowledgments. This work was supported by ENDESA company, ERDF, and CICYT under Grant 1FD97-0118-C02-01. The computational time assigned by CESGA on the Fujitsu VPP300E is gratefully acknowledged.

REFERENCES

Alapaty, K., R. Mathur, and T. Odman, 1998: Intercomparison of spatial interpolation schemes for use in nested grid models. *Mon. Wea. Rev.,* **126,** 243–249.

Berkowicz, R., and L. P. Prahm, 1982: Evaluation of the profile method for estimation of surface fluxes of momentum and heat. *Atmos. Environ.,* **16,** 2809–2819.

Blackadar, A. K., 1979: High resolution models of the planetary boundary layer. *Adv. Environ. Sci. Eng.,* **1,** 50–85.

Chen, J. H., 1973: Numerical boundary conditions and computational modes. *J. Comput. Phys.,* **13,** 522–535.

Daley, R., 1981: Normal mode initialization. *Rev. Geophys. Space Phys.,* **19,** 450–468.

Davies, H. C., 1983: Limitations of some common lateral boundary schemes used in regional NWP models. *Mon. Wea. Rev.,* **111,** 1002–1012.

Deardorff, J. W., 1974: Three-dimensional numerical study of the height and mean structure of a heated planetary boundary layer. *Bound.-Layer Meteor.,* **7,** 81–106.

——, 1978: Efficient prediction of ground surface temperature and moisture, with inclusion of a layer of vegetation. *J. Geophys. Res.,* **83,** 1889–1903.

Dudhia, J., D. Gill, Y. Guo, K. Manning, W. Wang, and J. Chiszar, 2000: Tutorial class notes and user's guide: MM5 Modeling System version 3. PSU/NCAR Mesoscale Modeling System, 381 pp.

Enger, L., 1990: Simulation of dispersion in moderately complex terrain. Part A. The fluid dynamic model. *Atmos. Environ.,* **24A,** 2431–2446.

Gimson, N. R., 1997: Pollution transport by convective clouds in a mesocale model. *Quart. J. Roy. Meteor. Soc.,* **123,** 1805–1828.

Goodin, W. R., G. J. McRae, and J. H. Seinfield, 1979: A comparison of interpolation methods for sparse data: Application to wind and concentration fields. *J. Appl. Meteor.,* **18,** 761–771.

Haltiner, G. J., and R. T. Williams, 1980: *Numerical Prediction and Dynamic Meteorology*. John Wiley and Sons, 450 pp.

Källen, E., Ed.,1996: HIRLAM documentation manual, system 2.5. 120 pp. [Available from Erland Källen, SMHI, S-601 79 Norrkoping, Sweden.]

Ludwig, F. L., R. J. Calhoun, R. T. Cederwall, and R. L. Street, 1999: Evaluation of vector interpolation methods for use with atmospheric boundary layer observations and simulations. Preprints, *13th Symp. on Boundary Layers and Turbulence*, Dallas, TX, Amer. Meteor. Soc., 320–323.

Mathur, R., and L. K. Peters, 1990: Adjustment of wind fields for application in air pollution modelling. *Atmos. Environ.,* **24A,** 1095–1106.

McCumber, M. C., and R. A. Pielke, 1981: Simulations of the effects of surface fluxes of heat and moisture in a mesoscale numerical model. Part I: Soil layer. *J. Geophys. Res.,* **86,** 9929–9938.

O'Brien, J. J., 1970: A note on the vertical structure of the eddy exchange coefficient in the planetary boundary layer. *J. Atmos. Sci.,* **27,** 1213–1215.

Pérez-Muñuzuri, V., 1998: Forecasting of chaotic cloud absorption time series for meteorological and plume dispersion modeling. *J. Appl. Meteor.,* **37,** 1430–1443.

——, and I. R. Gelpi, 2000: Application of nonlinear forecasting techniques for meteorological modeling. *Ann. Geophys.,* **18,** 1349–1359.

Perkey, D. J., and C. W. Kreitzberg, 1976: A time-dependent lateral boundary scheme for limited area primitive equation models. *Mon. Wea. Rev.,* **104,** 744–755.

Pielke, R. A., 1984: *Mesoscale Meteorological Modeling*. Academic Press, 612 pp.

——, and C. L. Martin, 1981: The derivation of a terrain-following coordinate system for use in a hydrostatic model. *J. Atmos. Sci.,* **38,** 1707–1713.

San José, R., 1991: A simple approach to evaluate mixed layer depths. *Environ. Software*, **6,** 161–167.

Shapiro, M. A., and J. J. O'Brien, 1970: Boundary conditions for fine-mesh limited-area forecasts. *J. Appl. Meteor.,* **9,** 345–349.

Smeda, M. S., 1979: Incorporation of planetary boundary layer processes into numerical forecasting models. *Bound.-Layer Meteor.,* **16,** 115–129.

Souto, J. A., V. Pérez-Muñuzuri, M. DeCastro, J. J. Casares, and J. Abadía, 1996: Application of short and 24 hours air pollution forecasting around a power plant. *Air Pollution IV. Monitoring, Simulation and Control*, B. Caussade, H. Power, and C. A. Brebbia, Eds., Computational Mechanics, 21–30.

——, ——, ——, M. J. Souto, J. J. Casares, and T. Lucas, 1998: Forecasting and diagnostic analysis of plume transport around a power plant. *J. Appl. Meteor.,* **37,** 1068–1083.

Souto, M. J., V. Pérez-Muñuzuri, J. A. Souto, M. DeCastro, and J. J. Casares, 1999: Forecasting of plume dispersion around a power plant. *Mixing and Dispersion in Stably Stratified Flows*, P. A. Davies, Ed., Clarendon Press, 455–475.

——, J. A. Souto, V. Pérez-Muñuzuri, J. J. Casares, and J. L. Bermúdez, 2001: A comparison of operational Lagrangian particle and adaptive puff models for plume dispersion forecasting. *Atmos. Environ.,* **35,** 2349–2360.

Tag, P. M., F. W. Murray, and L. R. Koenig, 1979: A comparison of several forms of eddy viscosity parameterization in a two-dimensional cloud model. *J. Appl. Meteor.,* **18,** 1429–1441.

Warner, T. T., R. A. Peterson, and R. E. Treadon, 1997: A tutorial on lateral boundary conditions as a basic and potentially serious limitation to regional numerical weather prediction. *Bull. Amer. Meteor. Soc.,* **78,** 2599–2617.